

See discussions, stats, and author profiles for this publication at: <https://www.researchgate.net/publication/228854700>

Insertion of a Two-Dimensional Cavity into a Self-Assembled Colloidal Crystal

ARTICLE *in* LANGMUIR · MAY 2003

Impact Factor: 4.46 · DOI: 10.1021/la0341916

CITATIONS

83

READS

23

7 AUTHORS, INCLUDING:



Kurt Wostyn

imec Belgium

69 PUBLICATIONS 1,221 CITATIONS

SEE PROFILE



Yuxia Zhao

Technical Institute of Physics and Chemistry

60 PUBLICATIONS 1,127 CITATIONS

SEE PROFILE



André Persoons

University of Leuven

245 PUBLICATIONS 8,105 CITATIONS

SEE PROFILE

Insertion of a Two-Dimensional Cavity into a Self-Assembled Colloidal Crystal

Kurt Wostyn,[†] Yuxia Zhao,[†] Gaetan de Schaetzen,[†] Louis Hellemans,[†]
Naoki Matsuda,[‡] Koen Clays,^{*,†} and André Persoons[†]

Laboratory of Chemical and Biological Dynamics, Department of Chemistry, University of Leuven, Celestijnenlaan 200D, B-3001 Leuven, Belgium, and Nanoarchitectonics Research Center (NARC), Tsukuba Central 5, 1-1-1 Higashi, Tsukuba, Ibaraki 305-8565, Japan

Received February 4, 2003. In Final Form: February 26, 2003

A planar microcavity has been inserted into a self-assembled colloidal crystal by a combination of convective self-assembly in a vertical geometry and the Langmuir–Blodgett technique. This planar cavity, which is parallel to the {111} planes, induces the appearance of a localized state, a pass band, into the forbidden band gap. We have experimentally determined the optical properties of this defect. The dependence of the position of the localized state is investigated as a function of the thickness of the defect layer. It is found that the defect behaves as a donor impurity, as it originates in the conduction band. Analogously, the crystal surrounding a constant defect layer can be varied. It is also found that the pass band depends on the thickness of the surrounding crystal of the planar defect.

Introduction

Since the pioneering works of Yablonovitch¹ and John,² there has been a growing interest in photonic crystals. Self-assembled crystals formed by spheres—mostly silica and polystyrene—are some of the systems that have been receiving much attention due to their ease of fabrication. A number of techniques have been developed since then in order to obtain high quality crystals, such as gravitational sedimentation,³ deposition using a specially designed cell,⁴ electrophoretic deposition,⁵ and vertical deposition using convective self-assembly.⁶ Colloidal crystals, regardless of the refractive index difference, will never produce a band gap covering all three dimensions.⁷ Inversion of the refractive index contrast is required.⁸ The voids between the spheres have been filled with silicon, and the spheres have been etched away.^{9,10} Recently, a full three-dimensional band gap has been proven in these crystals.¹¹ However, to guide light and for most foreseen applications such as low-threshold lasers, defects have to be introduced into these crystals. Only recently a start has been made to try to engineer defects into self-assembled structures. Point defects have been introduced by doping a colloidal crystal with impurity spheres of

different optical volume.¹² Braun et al. used two-photon photopolymerization to introduce waveguide structures into self-assembled photonic band gap materials.¹³ Also conventional lithographic methods have been used to introduce defects into inverted opal structures.¹⁰ We recently proposed a method to introduce a two-dimensional planar defect into synthetic opal¹⁴ by a combination of convective self-assembly in a vertical geometry,⁶ which has been shown to provide high quality crystals with a uniform thickness over large areas, and the Langmuir–Blodgett (LB) technique, which can be used to deposit a single layer of spheres.^{15,16} By successively depositing a multilayer crystal using convective self-assembly and then depositing a single layer using the LB technique and, finally, again depositing a multilayer using convective self-assembly, we succeeded in introducing a microcavity into a self-assembled crystal. Experimental investigation of the dependence of the position of the impurity mode on the thickness of the defect layer allows us to qualify the observed impurity mode as a donor or acceptor mode depending on the origin of the defect. Furthermore, we are able to observe a similar effect by changing the thickness of the surrounding crystal and keeping the thickness of the defect layer constant.

Experimental Section

Monodisperse silica spheres were synthesized following the Stöber–Fink–Bohn method through strict control of the reaction conditions.¹⁷ Absolute ethanol (Fluka) is mixed with ammonia (25%, Riedel-de-Haen) and deionized water (Milli-Q system). Tetraethyl orthosilicate (Aldrich) is added under vigorous stirring and left to react for at least 12 h. All glass reaction vessels were

* Corresponding author. E-mail: koen.clays@fys.kuleuven.ac.be.

[†] Laboratory of Chemical and Biological Dynamics, University of Leuven.

[‡] Nanoarchitectonics Research Center, Japan.

(1) Yablonovitch, E. *Phys. Rev. Lett.* **1987**, *58*, 2059.

(2) John, S. *Phys. Rev. Lett.* **1987**, *58*, 2486.

(3) Wijnhoven, J.; Vos, W. L. *Science* **1998**, *281*, 802.

(4) Gates, B.; Qin, D.; Xia, Y. *Adv. Mater.* **1999**, *11*, 466.

(5) Holgado, M.; Garcia-Santamaria, F.; Blanco, A.; Ibisate, M.; Cintas, A.; Miguez, H.; Serna, C. J.; Molpeceres, C.; Requena, J.; Mifsud, A.; Meseguer, F.; Lopez, C. *Langmuir* **1999**, *15*, 4701–4704.

(6) Jiang, P.; Bertone, J. F.; Hwang, K. S.; Colvin, V. L. *Chem. Mater.* **1999**, *11*, 2132.

(7) Biswas, R.; Sigalas, M. M.; Subramania, G.; Ho, K.-M. *Phys. Rev. B* **1998**, *57*, 3701.

(8) Busch, K.; John, S. *Phys. Rev. E* **1998**, *58*, 3896–3908.

(9) Blanco, A.; Chomski, E.; Grubbs, S.; Ibisate, M.; John, S.; Leonard, S. W.; Lopez, C.; Meseguer, F.; Miguez, H.; Mondia, J. P.; Ozin, G. A.; Toader, O.; van Driel, H. M. *Nature* **2000**, *405*, 437.

(10) Vlasov, Y. A.; Bo, X.-Y.; Sturm, J. C.; Norris, D. J. *Nature* **2001**, *414*, 289–293.

(11) Palacios-Lidon, E.; Blanco, A.; Ibisate, M.; Meseguer, F.; Lopez, C.; Sanchez-Dehesa, J. *Appl. Phys. Lett.* **2002**, *81*, 4925–4927.

(12) Pradhan, R. D.; Tarhan, I. I.; Watson, G. H. *Phys. Rev. B* **1996**, *54*, 13721.

(13) Lee, W.; Pruzinsky, A.; Braun, P. V. *Adv. Mater.* **2002**, *14*, 271–274.

(14) Zhao, Y.; Wostyn, K.; de Schaetzen, G.; Clays, K.; Hellemans, L.; Persoons, A.; Szekeres, M.; Schoonheydt, R. A. Submitted to *Appl. Phys. Lett.*

(15) van Duffel, B.; Ras, R. H. A.; De Schryver, F. C.; Schoonheydt, R. A. *J. Mater. Chem.* **2001**, *11*, 3333–3336.

(16) Szekeres, M.; Kamalin, O.; Schoonheydt, R. A.; Wostyn, K.; Clays, K.; Persoons, A.; Dekany, I. *J. Mater. Chem.* **2002**, *12*, 3268–3274.

(17) Stober, W.; Fink, A.; Bohn, E. *J. Colloid Interface Sci.* **1968**, *26*, 62–69.

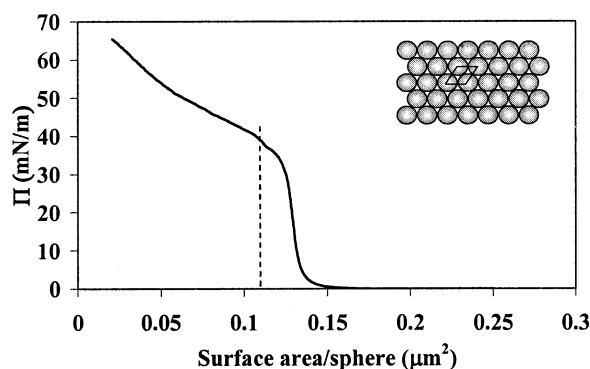


Figure 1. Surface area/surface pressure isotherm for 335 nm large spheres. The inset shows the hexagonal close packing of spheres. A unit cell is indicated. The theoretical surface area for which the LB film collapses is indicated using a dashed line.

cleaned extensively using hydrofluoric acid (Baker) and rinsed with water and ethanol prior to use. The colloidal suspension is then purified by repeated centrifugation, removal of supernatant, and redispersion in ethanol. The size of the colloids was obtained from dynamic light scattering measurements (Malvern Autosizer 4800) and confirmed by atomic force microscopy (Digital Instruments Dimension 3000).

The colloidal crystals were deposited on a glass substrate by convective self-assembly in a vertical geometry.⁶ This method allows for controlling of the number of layers in the colloidal crystal by adjusting the concentration of the colloidal suspension. A 3% stock solution of 290 nm large silica spheres is transferred to a flask, the solution is diluted to approximately 0.3%, and a glass slide is inserted. The flask is put in an oven at 32 °C. The crystal is grown to centimeter size over a period of 4 days. All glassware is cleaned using piranic acid (2/3 sulfuric acid (Acros), 1/3 20% hydrogen peroxide (Sigma)).

The middle single layer of silica spheres was made by the LB film method.^{15,16} For this, the fresh silica spheres are first dried and then dissolved into methanol to form a 3–4% solution. Surface area/surface pressure isotherms were recorded by spreading the methanolic solution onto the water surface at 20 °C (KSV Minitrough). After evaporation of the solvent, the monolayer of spheres was compressed at a speed of 5 mm/min (a typical example is shown in Figure 1). LB films were deposited using a KSV 5000 trough. An LB film was prepared as described above and compressed to a surface pressure of 20 mN/m. After stabilization for 30 min, the monolayer is transferred in upstroke to a glass slide or to the lower colloidal crystal. Scanning electron microscopy (SEM, Philips XL30 ESEM Feg) was used to determine the number of layers in the crystal and to show and check the quality of the colloidal crystal and sandwich structure. Optical density spectra ($-\log(\% \text{ transmission})$) were taken along the [111] crystallographic axis (perpendicular to the (111) planes), normal to the direction of the glass plate, using a Perkin-Elmer Lambda 900. The beam spot was 1 mm².

Results and Discussion

A typical surface area/surface pressure isotherm is shown in Figure 1. The LB film consists of 335 nm large spheres. The surface pressure starts to rise at approximately 0.15 μm² per sphere. The film collapsed at 0.125 μm² and a surface pressure of approximately 40 mN/m. The collapse could be observed visually as the occurrence of long white stripes on the surface. This method has been used to produce a two- and three-dimensional photonic band gap material.^{15,16} The inset shows a close packed layer of spheres. A unit cell is indicated. The unit cell contains one sphere, and the lattice constant equals the diameter of the spheres. For a film of close-packed spheres, the point of collapse should occur when the area per sphere is equal to the diameter of the spheres squared, as this would be the area occupied by one sphere in a close-packed arrangement of spheres. For

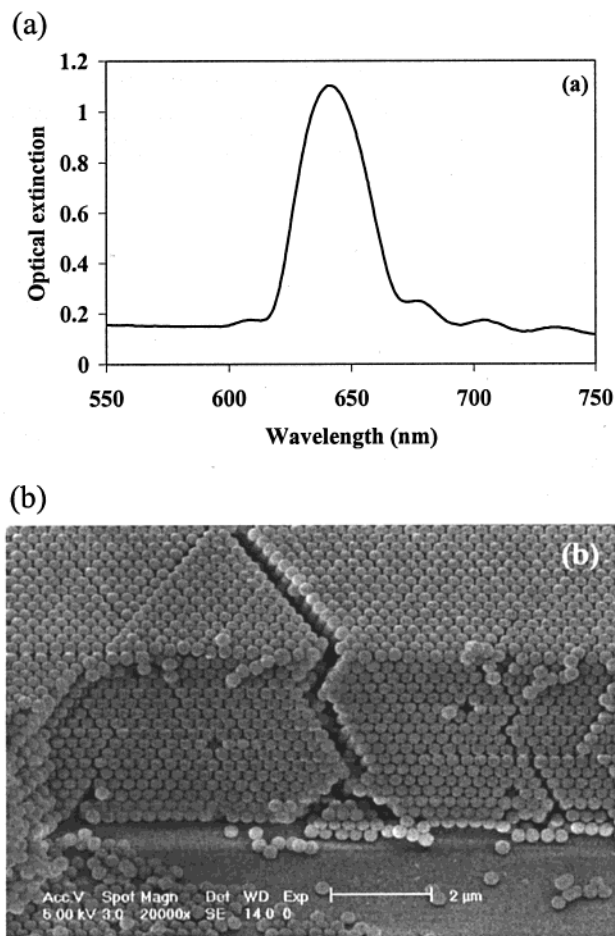


Figure 2. (a) Optical extinction spectrum and (b) an SEM image of an artificial opal consisting of 290 nm large spheres.

335 nm large spheres, this is at 0.112 μm² per sphere. The experimental point of collapse is somewhat higher than theoretically predicted. This can be explained by the occurrence of defects^{14–16} and even empty spots, that is, an area with no two-dimensional crystal and which can be observed visually, in the LB film.

Figure 2a shows the optical density spectrum obtained for a crystal of 290 nm large spheres. The Fabry–Perot fringes show that high quality crystals have been obtained. The Fabry–Perot fringes around the photonic band gap are mainly caused by the uniform thickness of the colloidal crystal. It is known that convective self-assembly leads to colloidal crystals with a uniform thickness. Figure 2b shows an SEM image of the crystal of 290 nm large silica spheres. Also here the good quality of the crystal can be observed. Photonic band gap materials can be seen as the optical analogues of semiconductors. In semiconductors, due to scattering of electrons on the crystal lattice, a band structure arises. This results in energy levels where no propagation of electrons is allowed. In photonic band gap materials, due to the scattering of photons on the crystal lattice, photonic band gaps appear. Also here, for some photon energies, or equivalently some range of wavelengths, no propagation of photons in a certain direction is allowed. In analogy to classical semiconductors, the allowed band at wavelengths above the photonic band gap could be called the valence band. The band at lower wavelengths could be called the conduction band.

Still analogous to semiconductors where, due to the insertion of impurity atoms, energy levels appear in the band gap, defect modes appear in the photonic band gap

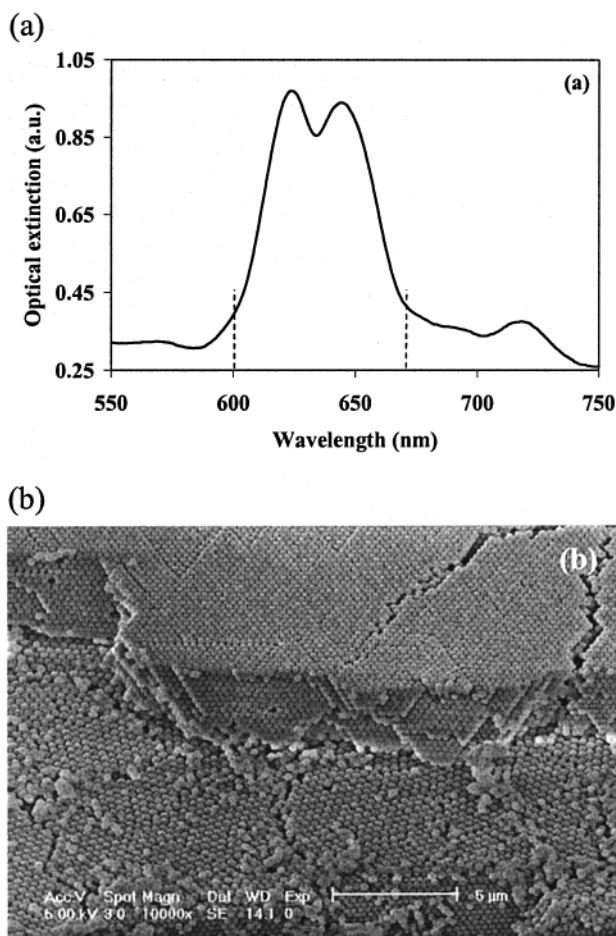


Figure 3. (a) Optical extinction spectrum and (b) an SEM image of a colloidal crystal consisting of 290 nm large spheres and 417 large spheres as a defect layer. The dashed lines in part a indicate the edges of the photonic band gap used in Figure 4.

when a defect of low dimensionality is inserted into the photonic band gap material. Such a defect may comprise a point (zero dimension, 0D); a line (1D); or a plane (2D). The insertion of a single layer of spheres with a different diameter produces such a 2D defect, and a “sandwich” structure arises. Figure 3a shows the optical density spectrum for the sandwich structure containing 417 nm large spheres as a middle single layer and 290 nm large spheres in the surrounding crystal. The spectrum shows a clear dip in the photonic band gap. A defect mode—a pass band—can be found in the photonic band gap that is caused by a state localized around the planar defect. Figure 3b shows a SEM image of this sandwich structure. The defect layer deposited using the LB technique surrounded by two layers of synthetic opal can be clearly seen.

Figure 4 shows the dependence of the position of the impurity mode on the defect size. The defect size here can be quantified by the diameter of the spheres making up the defect layer. Defects in photonic band gap materials lead to the occurrence of localized states in the forbidden region of the band gap.¹⁸ The perfect three-dimensional translational symmetry can be lifted in either one of two ways: (1) Extra dielectric material may be added to one of the unit cells, or some of the material may be replaced by material of a higher refractive index. Such a defect behaves very much like a donor atom in a semiconductor.

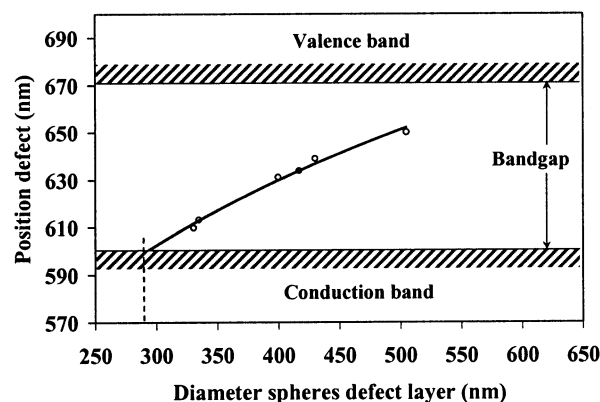


Figure 4. Influence of the thickness of the defect layer on the position of the impurity mode in the photonic band gap. The colloidal crystal consists of 290 nm large spheres. The edges of the photonic band gap have been taken from Figure 3a. The solid line does not represent a model and only serves as a guide to the eye. Note that the Y-axis represents wavelength instead of energy, so that the conduction band is below the valence band. On the energy axis, the conduction band is above the valence band.

It gives rise to donor modes which originate in the conduction band. (2) Conversely, the translational symmetry can be broken by removing some dielectric material from one of the unit cells or by replacing some of the material by material with a lower refractive index. Such defects resemble acceptor atoms in semiconductors. The associated acceptor modes have their origin in the valence band. The systematic shift in the position of the defect (see Figure 4) supports the fact that the observed changes in the photonic band gap are due to defect modes and are not caused by the superposition of different photonic band gaps on top of each other. The dependence of the position of the impurity mode on the defect size has been fitted to a phenomenological logarithmic function that does not represent any model and as such only serves as a guide to the eye. From this it can be seen that the defect modes arise in the conduction band and that defect modes can be expected to be observable from approximately 290 nm in size. This corresponds to the size of the upper and lower colloidal crystal. The insertion of a layer of 290 nm large silica spheres does not result in a defect, and so, no defect mode would be found. So, it can safely be concluded that the defect mode is a donor mode.

Instead of changing the diameter of the defect layer, alternatively, the size of the spheres of the surrounding colloidal crystal can be changed. Figure 5 shows the optical extinction spectra of a sandwich structure consisting of a defect layer of 415 nm large spheres and for which the surrounding crystal is made up of 280, 290, and 305 nm large silica spheres. It can be seen that the impurity mode shifts with increasing size of the spheres toward the conduction band. This is analogous to Figure 4, as increasing the size of the spheres in the surrounding crystal reduces the size of the defect layer relative to the size of the spheres in the surrounding synthetic opal. So again, we can conclude that the impurity mode originates in the conduction band and can be classified as a donor mode.

The impurity mode cannot be identified as clearly in every sample. This can be explained by a combination of three effects. The first effect is due to the imperfect nature of the engineered 2D defect. As can be seen from SEM images of LB films and deduced from the surface area/surface pressure isotherm, a number of imperfections (0D and 1D defects in the 2D layer) exist in the middle layer.

(18) Yablonovitch, E.; Gmitter, T. J.; Meade, R. D.; Rappe, A. M.; Brommer, K. D.; Joannopoulos, J. D. *Phys. Rev. Lett.* **1991**, *67*, 3380.

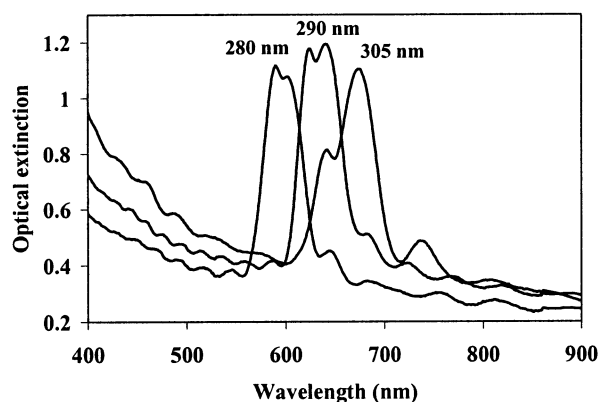


Figure 5. Optical extinction spectra for sandwich structures consisting of 415 nm large spheres for the defect layer and 280, 290, and 305 nm large spheres for the surrounding colloidal crystal.

This causes the 2D intentional defect to occur at different positions in the band gap for different areas of the sample. Averaging over the different areas then still leads to the observation of a pass band, but with a reduced contrast. A second contribution comes from the fact that defect modes become less apparent at the edges of a band gap and additionally the amplitude of the defect mode decreases exponentially when going away from the defect.¹⁹ This alters the appearance of the pass band with increasing thickness of the surrounding crystal. Figure 6 shows the optical density spectra of two crystals with different thickness of the surrounding crystal and the same defect layer deposited. From the spectra it can be seen that with increasing thickness the width of the band gap decreases. This has been observed previously for defect-free self-assembled colloidal crystals.²⁰ The appearance of the defect mode changes also. The thin crystal, as opposed to the thick crystal, shows a much clearer and deeper pass band. This can be explained by the exponentially decreasing amplitude of an impurity mode around a defect. For a thin crystal, the amplitude of the defect mode will still be large at the edges of the crystal, as opposed to the case of a thick crystal. This will lead to a larger leakage of the defect mode and as a result a larger transmission (lower optical extinction). A combination of

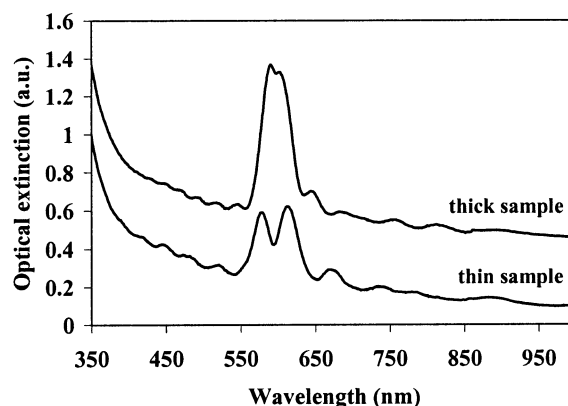


Figure 6. Influence of the thickness of the colloidal crystal on the impurity mode for a colloidal crystal of 280 nm large spheres and a defect layer of 415 nm large silica spheres. The “thick” crystal consists of approximately 21 layer thick colloidal crystals surrounding the defect layer. For the thin crystal, the surrounding colloidal crystals are 12 layers thick.

these effects explains why the impurity mode cannot be found as clearly in every sample. We are working on a numerical approach in order to model and quantify the observations in detail.

Conclusion

In summary, we have engineered a two-dimensional defect into a self-assembled photonic crystal. Using the Langmuir–Blodgett technique, we were able to transfer a monolayer of silica spheres to a self-assembled colloidal crystal. The deposition of an additional colloidal crystal on top of the single layer allows for the insertion of a 2D defect layer into a self-assembled crystal. The defect results in the observation of a pass band in the photonic band gap. The position of the defect was studied experimentally as a function of the thickness of the defect layer, and it was shown to behave as a donor mode. The same could be concluded from changing the spheres in the surrounding crystal and keeping the size of the defect constant. It has also been shown that the appearance of the defect mode changes with the thickness of the crystal.

Acknowledgment. KW is a research assistant supported by the Fund for Scientific Research–Flanders (FWO–V). This research was supported by grants of the Belgian Government (IUAP/5/3), the Fund for Scientific Research–Flanders (G.0261.02), and the University of Leuven (GOA/2000/03).

LA0341916

(19) Joannopoulos, J. D.; Meade, R. D.; Winn, J. N. *Photonic crystals: Molding the flow of light*, 1st ed.; Princeton University Press: Princeton, NJ, 1995; p 137.

(20) Mittleman, D. M.; Bertone, J. F.; Jiang, P.; Hwang, K. S.; Colvin, V. L. *J. Chem. Phys.* **1999**, *111*, 345.